1000-0569/2013/029(01)-0283-93 *Acta Petrologica Sinica* 岩石学报

福建紫金山矿田罗卜岭铜钼矿化斑岩锆石 LA-ICP-MS U-Pb 年龄及成矿岩浆高氧化特征研究*

黄文婷[1,2] 李晶[1,3] 梁华英[1**] 王春龙[1,2] 林书平[1,2] 王秀璋[1]

HUANG WenTing[1,2], LI Jing[1,3], LIANG HuaYing[1**], WANG ChunLong[1,2], LIN ShuPing[1,2] and WANG XiuZhang[1]

1. 中国科学院广州地球化学研究所,中国科学院矿物学与成矿学重点实验室,广州 510640
2. 中国科学院大学,北京 100049
3. 紫金矿业集团股份有限公司,上杭 364200

1. *Key Laboratory of Mineralogy and Metallogeny, Guangzhou Institute of Geochemistry, CAS, Guangzhou* 510640, *China*
2. *University of Chinese Academy of Sciences, Beijing* 100049, *China*
3. *Zijin Mining Group Co., Ltd, Shanghang* 364200, *China*

2012-04-05 收稿, 2012-11-25 改回.

Huang WT, Li J, Liang HY, Wang CL, Lin SP and Wang XZ. 2013. Zircon LA-ICP-MS U-Pb ages and highly oxidized features of magma associated with Luoboling porphyry Cu-Mo deposit in Zijinshan ore field, Fujian Province. *Acta Petrologica Sinica*, 29(1): 283 – 293

Abstract The Luoboling large porphyry Cu-Mo deposit is a recently discovered deposit in the Zijinshan Cu-Au-Mo ore field. Based on the relationship of the porphyries and the systematically petrographic study, the ore-bearing porphyries can be divided into early stage hornblende biotite granodiorite porphyry and biotite granodiorite porphyry and late stage biotite granodiorite porphyry. The early stage hornblende biotite granodiorite porphyry and biotite granodiorite porphyry has zircon LA-ICP-MS U-Pb age of 103.7 ± 1.2Ma, with MSWD = 0.33 and of 103.0 ± 0.9Ma with MSWD = 1.00, respectively, and the late stage biotite granodiorite porphyry has zircon LA-ICP-MS U-Pb age of 97.6 ± 2.1Ma with MSWD = 6.00. Zircon grains from two stage ore bearing porphyries have much higher average Ce^{4+}/Ce^{3+} ratios (630 ~ 770) than those (182 ~ 577) of barren granites in the ore field. Based on the zircon high Ce^{4+}/Ce^{3+} ratios and the wide occurrence of anhydrite in the ore-bearing porphyries, it is concluded that the ore-bearing magma was characterized by a relatively high oxygen fugacity. According to emplaced age and high oxygen fugacity of ore forming magma, and tectonic setting of the South China in the Mesozoic, the Luoboling ore-bearing porphyries are regarded to be triggered by the westward subduction of paleo-Pacific plate during Mesozoic.

Key words Porphyry Cu-Mo deposit; Mineralization age; Granodiorite porphyry; Zijinshan

摘 要 罗卜岭斑岩铜钼矿床是紫金山 Cu-Au-Mo 浅成低温-斑岩矿田内新近发现的大型斑岩铜钼矿床,本文在岩芯及光薄片系统观察的基础上,分析了矿化斑岩锆石 LA-ICP-MS U-Pb 年龄及锆石 Ce^{4+}/Ce^{3+} 比值。罗卜岭赋矿斑岩体可分为两期,早期为角闪黑云母花岗闪长斑岩及黑云母花岗闪长斑岩,晚期为黑云母花岗闪长斑岩。早期角闪黑云母花岗闪长斑岩和黑云母花岗闪长斑岩锆石 LA-ICP-MS U-Pb 年龄分别为 103.7 ± 1.2Ma,MSWD = 0.33 和 103.0 ± 0.9Ma,MSWD = 1.00;晚期黑云母花岗闪长斑岩锆石 LA-ICP-MS U-Pb 年龄为 97.6 ± 2.1Ma,MSWD = 6.00。罗卜岭成矿斑岩基质普遍发育硬石膏,两期成矿斑岩锆石都具较高的 Ce^{4+}/Ce^{3+} 平均值,在 630 ~ 770 之间,高于区内非成矿花岗岩锆石的 Ce^{4+}/Ce^{3+} 平均值(182 ~ 577),显示罗卜岭斑岩矿床成矿岩浆具有高氧逸度的特征。据罗卜岭斑岩矿床的形成时代、高氧逸度岩浆特征,结合华南地区中生代构造背景,我们初步认为罗卜岭斑岩矿床的形成可能和中生代古太平洋向北西西方向俯冲有关。

* 本文受中国科学院重大项目(KZCX1-YW-15-3)、中国科学院重点国际合作项目(GJHZ1127)、国家自然科学基金项目(41172080、41121002、41272099)和国土资源部深部矿产资源立体探测技术及实验研究项目(SinoProbe-03-01)联合资助.

第一作者简介: 黄文婷,女,1987 年生,博士生,矿床学专业,E-mail: ita19@163.com

** 通讯作者: 梁华英,男,1962 年生,研究员,博士生导师,矿床地质及矿床地球化学专业,E-mail: lianghy@gig.ac.cn

关键词 斑岩铜钼矿床; 锆石 U-Pb 年龄; 花岗闪长斑岩; 紫金山
中图法分类号 P588.13; P597.3

1 引言

斑岩型矿床是 Cu、Mo 和 Au 的主要来源,具有重要的经济意义,一直是矿床领域的研究热点(Seedorff *et al.*, 2005; Richards *et al.*, 2009; Sillitoe, 2010)。世界级大型斑岩铜矿多分布于环太平洋岩浆弧成矿带,科学家们建立了岩浆弧背景下的斑岩矿床成矿模型(Sillitoe, 1972; Mitchell, 1973; Bowen and Gunatilaka, 1977; Richards, 2003)。我国大型斑岩矿床和重要矿集区多产于碰撞造山环境(陈衍景, 2002, 2013),例如,青藏高原冈底斯斑岩铜矿带及藏东玉龙斑岩铜矿带(Liang *et al.*, 2006, 2009; 陈衍景, 2002; 郑有业等, 2002; 侯增谦等, 2003; 芮宗瑶等, 2006)、秦岭钼矿带(Chen *et al.*, 2000; 李诺等, 2007)、中亚成矿域的多金属矿床(Chen *et al.*, 2012; 陈衍景, 2000; 祁进平等, 2005; 陈衍景等, 2012)。我国学者对碰撞环境斑岩矿床开展了深入研究,建立了碰撞造山环境斑岩矿床成矿模式(陈衍景和富士谷, 1992; Chen, 1997; Chen *et al.*, 2000, 2004, 2007, 2012),并初步揭示了岩浆弧与大陆碰撞体制斑岩矿床的差异(陈衍景等, 2007; 陈衍景和李诺, 2009)。近年,我国华南斑岩矿床找矿工作取得了重大进展,除华南最大的德兴斑岩铜金矿床外,在粤北发现了园珠顶大型斑岩铜钼矿床、大宝山大型斑岩钼矿床及福建紫金山浅成低温热液矿田的罗卜岭大型斑岩铜(钼)矿床(钟军等, 2011)。然而,关于华南这些斑岩矿床的成矿构造环境,则有两种观点,即大陆碰撞(Chen *et al.*, 2007; 陈衍景, 2002)和洋陆俯冲(Zhou and Li, 2000; Sun *et al.*, 2007)。

紫金山斑岩-浅成低温热液成矿系统矿床类型齐全,发育有高硫型浅成低温热液 Cu-Au 矿床、低硫型 Ag 多金属矿床及斑岩型 Cu-Mo-(Au)矿床。过去研究工作多集中在紫金山浅成低温热液矿床上(So *et al.*, 1997; 张德全等, 1992, 2001, 2003, 2005; 华仁民等, 1998, 2002; 王少怀等, 2009; 陈静等, 2011),而对罗卜岭斑岩矿床研究工作相对薄弱,钟军等(2011)开展流体包裹体研究,张德全等(2001)对成矿花岗闪长斑岩进行了全岩 Rb-Sr 等时线定年,获得岩体年龄为 105±7Ma。目前,罗卜岭铜钼矿床含矿岩体的岩浆活动期次、成矿岩浆特征及其与斑岩型、浅成低温热液型矿化的关系等均待研究查明。这一工作直接影响着对紫金山斑岩-浅成低温热液矿田成矿系统形成机制的认识以及华南地区类似成矿系统的找矿部署。

本文在对罗卜岭赋矿斑岩体详细的镜下观察的基础上,

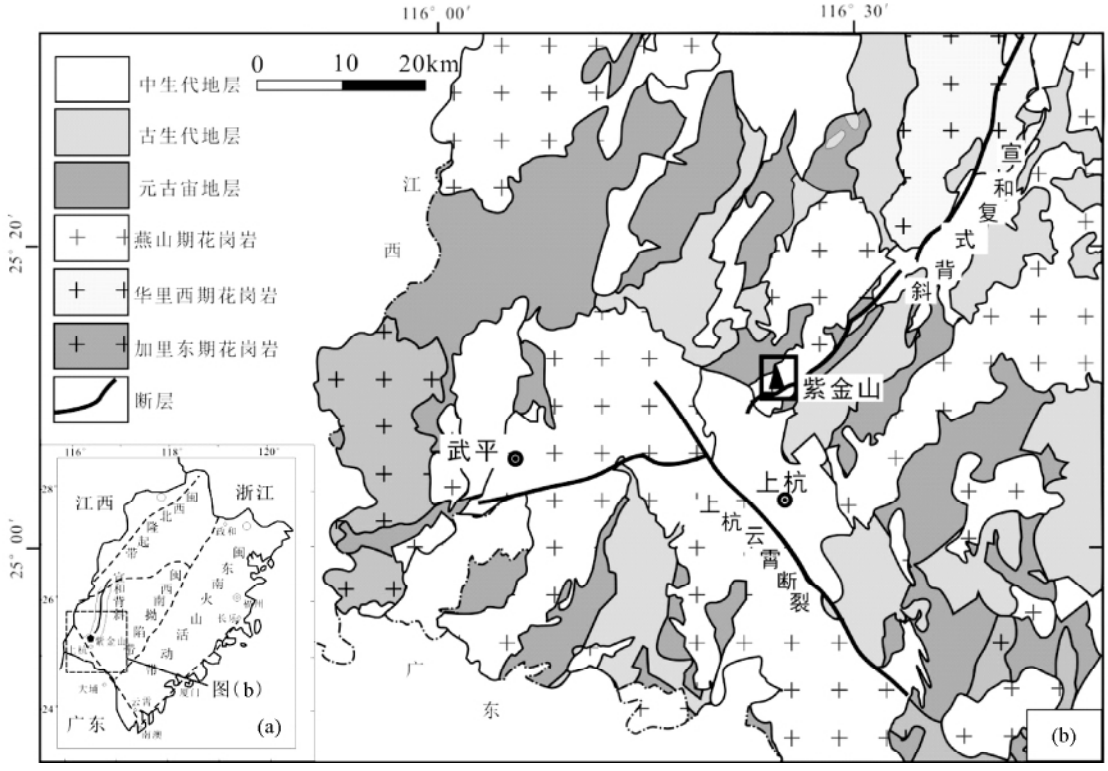

图 1 区域地质图(据福建省地质矿产局, 1985 修改)

Fig. 1 Regional geological map (modified after BGMRF, 1985)

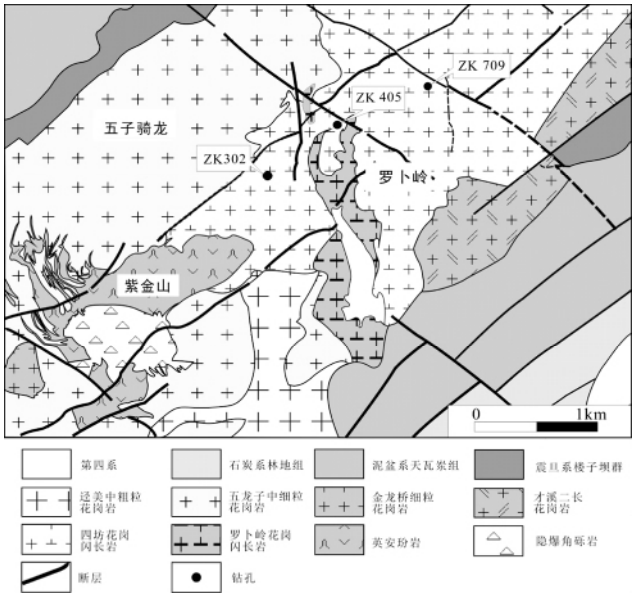

图 2　罗卜岭斑岩矿床地质简图(据钟军等, 2011 修改)

Fig. 2　Simplified geological map of the Luoboling porphyry Cu-Mo deposit (modified after Zhong *et al.*, 2011)

测定了矿化斑岩的锆石 LA-ICP-MS U-Pb 年龄,分析了成矿岩浆的特征。

2　罗卜岭斑岩矿床区域地质及矿床地质特征

福建省上杭县紫金山矿田位于西太平洋成矿带,华南褶皱带内,闽西南古生代坳陷带西南(图 1a),北东向宣和复式背斜与北西向上杭-云霄深断裂带的交汇部位(图 1b)。

紫金山矿田内出露地层主要有: 早震旦系楼子坝群、晚泥盆系天瓦崇组和桃子坑组、早石炭系林地组、早白垩系石帽山群及第四系。其中,楼子坝群为浅海相变质碎屑岩,天瓦崇组和桃子坑组为浅海-滨海相碎屑岩,石帽山群主要由英安质、粗安质、流纹质熔岩和火山碎屑岩组成,第四系主要为砂砾岩(图 2)。

矿区内构造以宣和复式背斜和断裂为主。宣和复式背斜呈北东向展布,主要由震旦系和古生代地层组成(图 1);断裂主要为北东向及北西向(图 2),其中北西向断裂为紫金山矿集区的重要的导矿和赋矿构造(薛凯和阮诗昆, 2008; 王少怀等, 2009)。

矿区内的燕山期岩浆活动强烈,主要出露岩体由早到晚分别为: 紫金山复式岩体(包括泾美中粗粒花岗岩,五龙子中细粒花岗岩和金龙桥细粒花岗岩)、才溪岩体、四坊岩体和罗卜岭斑岩体(图 2)。紫金山复式岩体位于矿田中部,形成于燕山晚期,锆石 SHRIMP U-Pb 年龄为 168 ± 4Ma(赵希林等, 2008);才溪中粗粒似斑状二长花岗岩出露于矿区北东部,呈北东向延伸,侵入于晚古生代地层中,锆石 SHRIMP U-Pb 年龄为 150 ± 3Ma(赵希林等, 2007);四坊中细粒花岗闪长岩侵入于紫金山复式岩体的东北部及才溪岩体的西南部,单颗粒锆石 U-Pb 年龄为 107.8 ± 1.2Ma(毛建仁等, 2002);罗卜岭花岗闪长斑岩体位于矿田中南部,呈钳状侵入于四坊岩体中,其 Rb-Sr 等时线年龄为 105 ± 7Ma(张德全等, 2001)。

罗卜岭斑岩体地表出露部分呈岩瘤状,面积约 0.20km^2(图 2),深部呈岩株形态(薛凯和阮诗昆, 2008)。矿区斑岩普遍发生蚀变,主要类型有硅化、钾化、绢云母化、绿泥石化、泥化、黄铁矿化等。矿体主要产于花岗闪长斑岩体的外接触带,赋存于绢云母化叠加钾化蚀变带和黄铁绢英岩化蚀变带中,矿化类型以铜钼为主,呈细脉浸染状及浸染状产于花岗闪长斑岩中; 主要金属矿物有: 黄铜矿、黄铁矿、斑铜矿及辉钼矿等。目前已控制铜金属含量超过 100Mt,平均品位 0.3%,钼金属资源超过 0.1Mt,平均品位 0.036%。

3　赋矿斑岩矿物组成特征

罗卜岭矿区地表植被较多,赋矿斑岩浅部风化蚀变较强。为分析罗卜岭斑岩矿床成矿岩体特征,我们在系统的岩芯观察的基础上,采集了 ZK405、ZK709、ZK802 等钻孔(图 2)中蚀变较弱的岩芯样品。手标本观察显示,矿化斑岩分为两类: 角闪黑云母花岗闪长斑岩和黑云母花岗闪长斑岩。在 ZK709 孔 870m 处观察到了晚期黑云母花岗闪长斑岩包裹早期黑云母花岗闪长斑岩(图 3a),表明黑云母花岗闪长斑岩为两期岩浆作用形成的。

角闪黑云母花岗闪长斑岩见于 ZK802 孔(图 3 b),镜下观察显示其斑晶主要为斜长石、角闪石、石英、黑云母、钾长石,基质主要为石英和钾长石,各矿物的相对含量详见表 1。岩石普遍发生钾硅化、绢云母化及绿泥石化。

早期黑云母花岗闪长斑岩见于 ZK405 孔(图 3 c),晚期黑云母花岗闪长斑岩见于 ZK709 孔(图 3 d)。在 76 个样品光薄片镜下观察的基础上,我们对 ZK405 孔 10 个及 ZK709 孔 6 个蚀变较弱黑云母花岗闪长斑岩的光薄片矿物组成统计分析(表 1)。结果表明早晚两期黑云母花岗闪长斑岩的矿物组成基本相同: 斑晶主要为斜长石、石英、黑云母和少量的钾长石,基质主要为石英和钾长石(图 3c, d)。但两者的斑晶矿物含量存在一定的差别(表 1)。主要表现在早期黑云母花岗闪长斑岩斑晶含量相对较少,在 20% ~35% 之间,而其中 53 ~83% 为斜长石斑晶; 晚期黑云母花岗闪长斑岩斑晶含量较高,在 38% ~44% 之间,而其中石英和钾长石斑晶含量较早期的高,斜长石斑晶含量较早期的低(表 1)。

值得一提的是硬石膏在矿化斑岩中普遍出现,主要呈两种形式产出: (1) 零星分布于基质中(图 3e),与其他矿物接触边界平坦,未见反应边,这和 Stern *et al.* (2007) 描述的岩浆期结晶析出的硬石膏特征相似,显示其是岩浆期形成的; (2) 分布于热液期石英-钾长石-硬石膏脉中(图 3f),与矿化关系密切,主要出现深度为 450 ~800m。

表 1 罗卜岭斑岩矿物含量(vol%)统计

Table 1 Statistics of mineral content (vol%) of the Luoboling porphyries

岩性	基质	斑晶	斑晶矿物相对含量				
			石英	斜长石	黑云母	钾长石	角闪石
早期角闪黑云母花岗闪长斑岩	30~50	50~70	13	60	10	2	15
早期黑云母花岗闪长斑岩	65~80	20~35	4~18	58~83	1.7~8.3	1.2~4.8	
晚期黑云母花岗闪长斑岩	56~62	38~44	38~43	28~63	4~11.3	5.6~22	

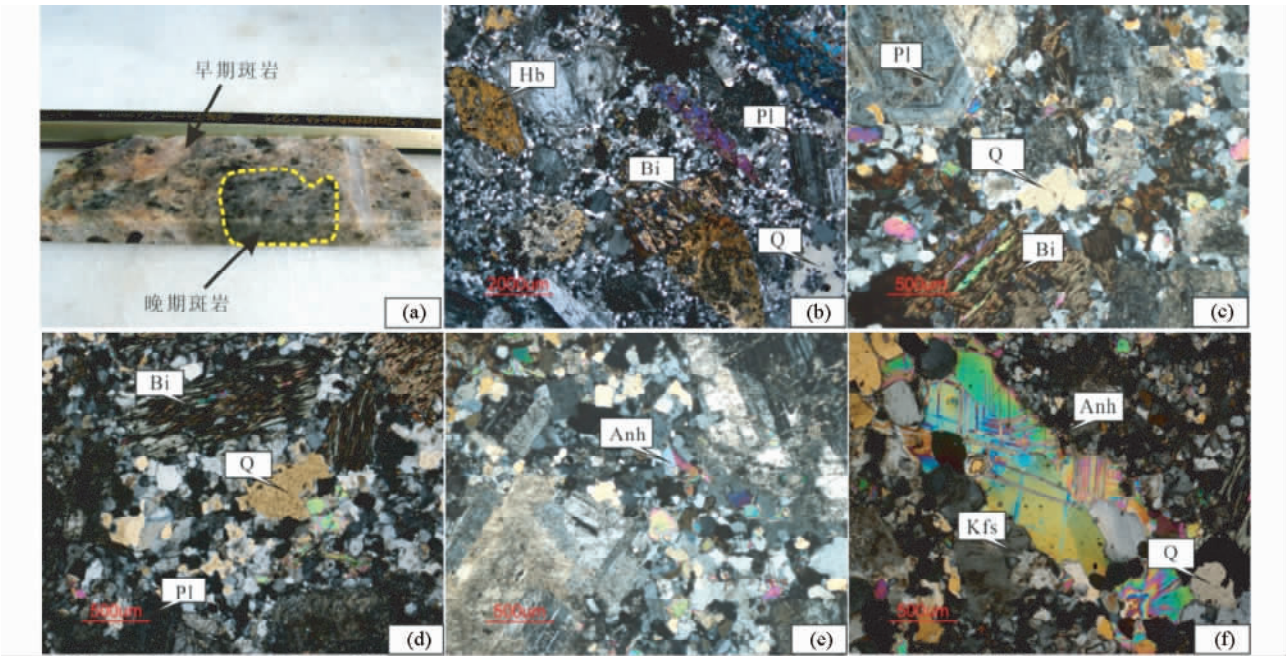

图 3 罗卜岭斑岩铜钼矿床两期矿化斑岩接触关系及矿物组合

(a)-罗卜岭两期黑云母花岗闪长斑岩的接触关系;(b)-ZK802 孔角闪黑云母花岗闪长斑岩矿物组合,斑晶为斜长石、角闪石、黑云母、石英,基质为石英和钾长石;(c)-ZK405 孔早期黑云母花岗闪长斑岩矿物组合,斑晶为斜长石、石英,黑云母,基质为石英和钾长石;(d)-ZK709 孔晚期黑云母花岗闪长斑岩矿物组合,斑晶为斜长石、石英、黑云母,基质为石英和钾长石;(e)-基质中零星分布的硬石膏,与周围矿物接触边界平坦,未见反应边,为岩浆期结晶形成;(f)-热液期的石英-钾长石-硬石膏脉. Pl-斜长石; Q-石英; Bi-黑云母; Hb-角闪石; Anh-硬石膏; Kfs-钾长石

Fig. 3 Photographs showing contact relationship of two stages biotite granodiorite porphyries and mineral assemblage of the Luoboling ore-bearing porphyries

(a)-photograph showing the relationship of two stages biotite granodiorite porphyries in Luoboling deposit; (b)-mineral assemblage of hornblende biotite granodiorite porphyry from ZK802. Phenocrysts include plagioclase, hornblende, biotite and quartz while the matrixes consist of quartz and feldspar; (c)-mineral assemblage of early stage biotite granodiorite porphyry from ZK405, the phenocrysts including plagioclase, quartz and biotite while the matrixes consist of quartz and feldspar; (d)-mineral assemblage of late stage biotite granodiorite porphyry from ZK709, the phenocrysts including plagioclase, quartz and biotite while the matrixes consist of quartz and feldspar; (e)-anhydrite distribute in the matrix. The crystal boundaries between anhydrite and other phases are planar, suggests that anhydrite is an igneous phase; (f)-the quartz-K-feldspar-anhydrite vein of the hydrotherma stage. Pl-plagioclase; Q-quartz; Bi-biotite; Hb-hornblende; Anh-anhydrite; Kfs-feldspar

4 测试方法与分析结果

锆石 LA-ICP-MS U-Pb 定年样品采自钻孔岩芯。其中早期黑云母花岗闪长斑岩(LBL-81)和晚期黑云母花岗闪长斑岩(LBL-132)分别采自 ZK405 孔 678m 处和 ZK709 孔 804m 处;角闪黑云母花岗闪长斑岩(LBL-203)采自 ZK802 孔 247m 处。

每个样品选取约 0.5kg 的岩石,研磨至 80 目,经筛选、淘选、磁选等处理后,在显微镜下手选出晶形完整的锆石 70~80 颗,装入环氧树脂中制成靶、磨光,在光学显微镜下选出

表 2　罗卜岭晚期黑云母花岗闪长斑岩(样品 LBL-132)锆石 LA-ICP-MS 分析结果

Table 2　Zircon LA-ICP-MS data of the Luoboling late stage biotite granodiorite porphyry (Sample LBL-132)

测点号	Pb	U	Th/U	Ce(IV)/Ce(III)	同位素比值								年龄(Ma)						谐和度
	($\times10^{-6}$)				$\frac{^{206}Pb}{^{238}U}$	$\pm1\sigma$	$\frac{^{207}Pb}{^{235}U}$	$\pm1\sigma$	$\frac{^{207}Pb}{^{206}Pb}$	$\pm1\sigma$	$\frac{^{208}Pb}{^{232}Th}$	$\pm1\sigma$	$\frac{^{207}Pb}{^{235}U}$	$\pm1\sigma$	$\frac{^{208}Pb}{^{232}Th}$	$\pm1\sigma$	$\frac{^{206}Pb^*}{^{238}U}$	$\pm1\sigma$	
LBL-132-01	25.0	1534.3	0.28	1529	0.01525	0.00035	0.10653	0.00755	0.05054	0.00360	0.00497	0.00025	102.8	6.9	100.1	4.9	97.6	2.2	94%
LBL-132-02	17.4	974.1	0.35	406	0.01634	0.00035	0.10990	0.00729	0.04865	0.00317	0.00504	0.00030	105.9	6.7	101.6	6.1	104.5	2.2	98%
LBL-132-03	19.7	1128.9	0.42	340	0.01532	0.00034	0.10064	0.00752	0.04772	0.00360	0.00505	0.00025	97.4	6.9	101.9	5.1	98.0	2.1	99%
LBL-132-04	20.8	1279.4	0.30	968	0.01472	0.00035	0.10277	0.00733	0.05049	0.00348	0.00526	0.00024	99.3	6.8	106.0	4.9	94.2	2.2	94%
LBL-132-05	23.9	1447.3	0.37	1642	0.01459	0.00031	0.10229	0.00767	0.05093	0.00371	0.00545	0.00029	98.9	7.1	109.8	5.9	93.4	2.0	94%
LBL-132-06	17.0	912.9	0.46		0.01616	0.00029	0.09304	0.00670	0.04191	0.00308	0.00475	0.00024	90.3	6.2	95.8	4.8	103.3	1.8	86% 剔除
LBL-132-07	18.3	970.6	0.40	184	0.01618	0.00030	0.11520	0.00762	0.05165	0.00343	0.00557	0.00027	110.7	6.9	112.3	5.5	103.5	1.9	93%
LBL-132-08	20.4	1181.4	0.42		0.01503	0.00032	0.11211	0.00922	0.05480	0.00472	0.00492	0.00020	107.9	8.4	99.2	4.0	96.2	2.0	88% 剔除
LBL-132-09	26.5	1294.3	0.93	832	0.01599	0.00040	0.11066	0.00731	0.04995	0.00305	0.00501	0.00018	106.6	6.7	101.0	3.6	102.3	2.5	95%
LBL-132-10	23.8	1376.4	0.31	980	0.01606	0.00037	0.11265	0.00763	0.05106	0.00350	0.00521	0.00023	108.4	7.0	105.0	4.5	102.7	2.4	94%
LBL-132-11	22.7	1304.9	0.28	1258	0.01609	0.00036	0.11314	0.00877	0.05049	0.00372	0.00509	0.00023	108.8	8.0	102.6	4.6	102.9	2.3	94%
LBL-132-12	30.5	1916.8	0.27	917	0.01441	0.00023	0.10257	0.00665	0.05100	0.00326	0.00533	0.00021	99.1	6.1	107.5	4.2	92.2	1.5	92%
LBL-132-13	24.4	1329.1	0.39	556	0.01633	0.00038	0.11273	0.00734	0.05011	0.00325	0.00575	0.00028	108.5	6.7	115.8	5.6	104.4	2.4	96%
LBL-132-14	28.3	1777.7	0.27	1469	0.01476	0.00031	0.09985	0.00592	0.04892	0.00295	0.00540	0.00027	96.6	5.5	108.8	5.5	94.4	2.0	97%
LBL-132-15	23.1	1457.4	0.25	176	0.01498	0.00032	0.09297	0.00637	0.04461	0.00305	0.00546	0.00028	90.3	5.9	110.0	5.7	95.9	2.1	93%
LBL-132-16	47.5	2962.8	0.37	680	0.01419	0.00023	0.09302	0.00575	0.04706	0.00300	0.00515	0.00025	90.3	5.3	103.9	4.9	90.8	1.5	99%
LBL-132-17	13.0	734.6	0.36	364	0.01596	0.00029	0.11138	0.00900	0.05040	0.00422	0.00511	0.00031	107.2	8.2	102.9	6.3	102.1	1.9	95%
LBL-132-18	25.4	1617.5	0.26	903	0.01471	0.00039	0.09983	0.00700	0.04817	0.00292	0.00581	0.00029	96.6	6.5	117.0	5.8	94.2	2.5	97%
LBL-132-19	33.0	2038.2	0.34	804	0.01437	0.00026	0.10270	0.00677	0.05092	0.00316	0.00521	0.00020	99.3	6.2	105.0	4.0	92.0	1.7	92%
LBL-132-20	13.2	719.1	0.28	264	0.01636	0.00032	0.11643	0.00752	0.05151	0.00339	0.00589	0.00029	111.8	6.8	118.8	5.9	104.6	2.0	93%
LBL-132-21	16.0	929.2	0.29	406	0.01559	0.00037	0.09572	0.00762	0.04540	0.00392	0.00525	0.00028	92.8	7.1	105.8	5.5	99.7	2.4	92%
LBL-132-22	18.6	1053.2	0.26	1100	0.01574	0.00027	0.11003	0.00772	0.05063	0.00366	0.00613	0.00031	106.0	7.1	123.5	6.1	100.7	1.7	94%
LBL-132-23	25.6	1529.2	0.34	859	0.01518	0.00036	0.10658	0.00657	0.05033	0.00288	0.00506	0.00021	102.8	6.0	102.1	4.2	97.1	2.3	94%
LBL-132-24	14.0	790.6	0.26	486	0.01592	0.00027	0.10728	0.00786	0.04864	0.00365	0.00603	0.00032	103.5	7.2	121.5	6.4	101.8	1.7	98%
LBL-132-25	21.9	1342.8	0.33	552	0.01441	0.00031	0.09516	0.00681	0.04736	0.00335	0.00544	0.00026	92.3	6.3	109.7	5.3	92.2	2.0	99%

表 3 罗卜岭早期黑云母花岗闪长斑岩(样品 LBL-81)锆石 LA-ICP-MS 分析结果

Table 3 Zircon LA-ICP-MS data of the Luoboling early stage biotite granodiorite porphyry (Sample LBL-81)

测点号	Pb ($\times10^{-6}$)	U ($\times10^{-6}$)	Th/U	Ce(IV)/Ce(III)	$^{206}Pb/^{238}U$	±1σ	$^{207}Pb/^{235}U$	±1σ	$^{207}Pb/^{206}Pb$	±1σ	$^{208}Pb/^{232}Th$	±1σ	$^{207}Pb/^{235}U$ 年龄(Ma)	±1σ	$^{208}Pb/^{232}Th$ 年龄(Ma)	±1σ	$^{206}Pb^{*}/^{238}U$ 年龄(Ma)	±1σ	谐和度
LBL-81-01	12.5	644.4	0.53	199	0.01603	0.00036	0.10880	0.01208	0.04943	0.00557	0.00463	0.00034	104.9	11.1	93.3	6.8	102.5	2.3	97%
LBL-81-02	11.4	595.8	0.47	390	0.01624	0.00038	0.09969	0.01052	0.04476	0.00475	0.00456	0.00031	96.5	9.7	92.0	6.3	103.8	2.4	92%
LBL-81-03	11.7	599.3	0.60	186	0.01560	0.00031	0.11030	0.01144	0.05117	0.00534	0.00465	0.00027	106.2	10.5	93.8	5.4	99.8	2.0	93%
LBL-81-04	12.7	654.3	0.50	612	0.01632	0.00037	0.11371	0.01171	0.05033	0.00515	0.00423	0.00028	109.4	10.7	85.4	5.6	104.4	2.3	95%
LBL-81-05	12.8	681.8	0.44	625	0.01566	0.00035	0.10276	0.01158	0.04708	0.00536	0.00425	0.00027	99.3	10.7	85.7	5.5	100.2	2.2	99%
LBL-81-06	11.6	598.2	0.49	407	0.01640	0.00044	0.11060	0.01278	0.04893	0.00572	0.00474	0.00031	106.5	11.7	95.6	6.2	104.9	2.8	98%
LBL-81-07	13.0	608.8	0.81	113	0.01662	0.00040	0.11089	0.01140	0.04844	0.00499	0.00469	0.00025	106.8	10.4	94.5	5.0	106.3	2.5	99%
LBL-81-08	10.7	519.3	0.69	192	0.01669	0.00038	0.10522	0.01221	0.04574	0.00517	0.00462	0.00024	101.6	11.2	93.3	4.8	106.7	2.4	95%
LBL-81-09	11.4	607.8	0.42	949	0.01618	0.00032	0.10090	0.00973	0.04515	0.00449	0.00465	0.00030	97.6	9.0	93.8	6.1	103.4	2.0	94%
LBL-81-10	11.9	645.6	0.41	665	0.01621	0.00039	0.10836	0.01105	0.04782	0.00477	0.00463	0.00029	104.5	10.1	93.3	5.8	103.7	2.5	99%
LBL-81-11	12.3	658.2	0.49	584	0.01604	0.00032	0.10744	0.00990	0.04881	0.00460	0.00492	0.00030	103.6	9.1	99.2	6.0	102.6	2.0	98%
LBL-81-12	14.1	757.3	0.43	802	0.01604	0.00029	0.10880	0.00839	0.04967	0.00391	0.00475	0.00025	104.9	7.7	95.9	5.1	102.6	1.8	97%
LBL-81-13	12.3	645.1	0.53	435	0.01615	0.00037	0.11259	0.01064	0.05131	0.00482	0.00509	0.00027	108.3	9.7	102.6	5.3	103.3	2.4	95%
LBL-81-14	11.2	575.3	0.40	625	0.01696	0.00042	0.10683	0.00997	0.04692	0.00459	0.00544	0.00034	103.1	9.1	109.6	6.8	108.4	2.7	94%
LBL-81-15	12.1	624.2	0.49	308	0.01660	0.00041	0.10412	0.01046	0.04687	0.00499	0.00518	0.00034	100.6	9.6	104.4	6.8	106.2	2.6	94%
LBL-81-16	13.6	708.5	0.54	380	0.01620	0.00034	0.10869	0.01194	0.04881	0.00521	0.00515	0.00030	104.8	10.9	103.8	6.1	103.6	2.2	98%
LBL-81-17	12.3	653.7	0.50	524	0.01591	0.00035	0.11680	0.01132	0.05466	0.00554	0.00500	0.00027	112.2	10.3	100.8	5.5	101.8	2.2	90%
LBL-81-18	12.2	659.8	0.46	823	0.01604	0.00040	0.09816	0.00911	0.04556	0.00433	0.00494	0.00030	95.1	8.4	99.7	6.1	102.6	2.6	92%
LBL-81-19	17.5	898.5	0.70		0.01632	0.00042	0.09501	0.00769	0.04396	0.00382	0.00519	0.00021	92.2	7.1	104.7	4.2	104.4	2.7	87% 剔除
LBL-81-20	6.2	348.7	0.29	3576	0.01601	0.00036	0.10722	0.01488	0.04960	0.00679	0.00475	0.00057	103.4	13.7	95.7	11.4	102.4	2.3	99%
LBL-81-21	10.0	571.2	0.35	787	0.01538	0.00039	0.09592	0.01006	0.04485	0.00448	0.00564	0.00048	93.0	9.3	113.6	9.6	98.4	2.5	94%
LBL-81-22	11.0	553.8	0.60	260	0.01641	0.00035	0.11359	0.01221	0.04960	0.00518	0.00543	0.00029	109.2	11.1	109.5	5.9	105.0	2.2	95%
LBL-81-23	13.1	735.3	0.34	970	0.01558	0.00030	0.10266	0.00988	0.04811	0.00484	0.00556	0.00034	99.2	9.1	112.1	6.8	99.6	1.9	99%
LBL-81-24	9.2	486.3	0.48	518	0.01605	0.00037	0.10851	0.01324	0.04984	0.00623	0.00485	0.00027	104.6	12.1	97.8	5.4	102.7	2.3	98%
LBL-81-25	10.4	533.5	0.50	182	0.01603	0.00038	0.11144	0.01606	0.05064	0.00758	0.00590	0.00034	107.3	14.7	118.8	6.8	102.5	2.4	95%

表 4　罗卜岭早期角闪黑云母花岗闪长斑岩(样品 LBL-203)锆石 LA-ICP-MS 分析结果

Table 4　Zircon LA-ICP-MS data of the Luoboling early stage hornblende biotite granodiorite porphyry (Sample LBL-203)

测点号	Pb	U	同位素比值										年龄(Ma)						谐和度
	($\times10^{-6}$)		Th/U	Ce(IV)/Ce(III)	$^{206}Pb/^{238}U$	±1σ	$^{207}Pb/^{235}U$	±1σ	$^{207}Pb/^{206}Pb$	±1σ	$^{208}Pb/^{232}Th$	±1σ	$^{207}Pb/^{235}U$	±1σ	$^{208}Pb/^{232}Th$	±1σ	$^{206}Pb^{*}/^{238}U$	±1σ	
LBL-203-01	13.3	651.5	0.49	1272	0.01613	0.00043	0.09846	0.01097	0.04324	0.00462	0.00468	0.00034	95.4	10.1	94.3	6.8	103.1	2.7	92%
LBL-203-02	15.5	726.6	0.54	1016	0.01645	0.00041	0.10852	0.01320	0.04814	0.00600	0.00513	0.00030	104.6	12.1	103.4	6.0	105.2	2.6	99%
LBL-203-03	13.2	655.3	0.37	205	0.01646	0.00045	0.10820	0.01542	0.04842	0.00684	0.00565	0.00054	104.3	14.1	113.9	10.9	105.3	2.8	99%
LBL-203-04	12.9	620.5	0.49	1344	0.01593	0.00035	0.10045	0.01241	0.04462	0.00549	0.00494	0.00038	97.2	11.5	99.6	7.6	101.9	2.2	95%
LBL-203-05	8.2	351.0	0.80	98	0.01709	0.00060	0.10808	0.02265	0.04717	0.01029	0.00522	0.00031	104.2	20.8	105.3	6.3	109.2	3.8	95%
LBL-203-06	4.8	158.8	0.81		0.01681	0.00084	0.12987	0.06428	0.04198	0.02567	0.01458	0.00143	124.0	57.8	292.5	28.4	107.4	5.3	85% 剔除
LBL-203-07	11.6	570.1	0.37	552	0.01592	0.00037	0.11179	0.01256	0.05013	0.00562	0.00539	0.00042	107.6	11.5	108.7	8.4	101.8	2.4	94%
LBL-203-08	12.3	589.7	0.47	444	0.01611	0.00036	0.10990	0.01326	0.04882	0.00574	0.00469	0.00032	105.9	12.1	94.7	6.4	103.0	2.3	97%
LBL-203-09	14.4	674.1	0.53	289	0.01613	0.00037	0.10620	0.01221	0.04764	0.00548	0.00542	0.00037	102.5	11.2	109.3	7.4	103.2	2.4	99%
LBL-203-10	10.6	525.5	0.46	856	0.01611	0.00046	0.10159	0.01456	0.04518	0.00625	0.00428	0.00036	98.2	13.4	86.3	7.3	103.0	2.9	95%
LBL-203-11	6.2	237.0	0.98	1214	0.01660	0.00068	0.10299	0.02346	0.04509	0.01007	0.00677	0.00051	99.5	21.6	136.5	10.2	106.1	4.3	93%
LBL-203-12	15.4	750.6	0.41	1269	0.01617	0.00047	0.10169	0.00997	0.04606	0.00463	0.00527	0.00040	98.3	9.2	106.2	8.0	103.4	3.0	94%
LBL-203-13	10.4	506.6	0.45	879	0.01655	0.00054	0.10023	0.01421	0.04410	0.00611	0.00480	0.00039	97.0	13.1	96.8	7.8	105.8	3.4	91%
LBL-203-14	10.8	544.0	0.42		0.01587	0.00043	0.09380	0.00942	0.04242	0.00413	0.00547	0.00041	91.0	8.7	110.3	8.3	101.5	2.8	89% 剔除
LBL-203-15	10.8	532.8	0.43	384	0.01658	0.00057	0.10751	0.01198	0.04916	0.00572	0.00499	0.00045	103.7	11.0	100.5	9.0	106.0	3.6	97%
LBL-203-16	15.4	768.7	0.47	455	0.01619	0.00044	0.10161	0.01137	0.04594	0.00522	0.00500	0.00040	98.3	10.5	100.8	8.1	103.6	2.8	94%
LBL-203-17	17.9	918.6	0.28	762	0.01628	0.00035	0.10506	0.01177	0.04682	0.00525	0.00516	0.00040	101.4	10.8	104.0	8.0	104.1	2.2	97%
LBL-203-18	14.2	720.0	0.30	521	0.01635	0.00044	0.10655	0.01071	0.04709	0.00463	0.00570	0.00043	102.8	9.8	115.0	8.7	104.6	2.8	98%
LBL-203-19	10.1	503.0	0.37	2461	0.01620	0.00040	0.11048	0.01410	0.04932	0.00641	0.00488	0.00045	106.4	12.9	98.4	9.1	103.6	2.5	97%
LBL-203-20	18.2	915.6	0.43	713	0.01593	0.00041	0.10836	0.01197	0.04876	0.00527	0.00438	0.00032	104.5	11.0	88.3	6.5	101.9	2.6	97%
LBL-203-21	9.7	472.4	0.46	387	0.01601	0.00041	0.11056	0.01885	0.04925	0.00843	0.00452	0.00035	106.5	17.2	91.1	7.0	102.4	2.6	96%
LBL-203-22	10.3	469.0	0.54	277	0.01627	0.00053	0.10573	0.01504	0.04858	0.00721	0.00530	0.00047	102.0	13.8	106.9	9.4	104.0	3.4	98%
LBL-203-23	13.9	704.2	0.53		0.01452	0.00040	0.11314	0.01388	0.05733	0.00735	0.00476	0.00029	108.8	12.7	95.9	5.8	93.0	2.5	84% 剔除

无裂纹且包裹体不发育的锆石晶体进行测定。锆石 LA-ICP-MS 定年在中国科学院广州地球化学研究所 ICP-MS 实验室完成,测试时使用 RESE(澳大利亚国立大学地质地球科学研究所)标准锆石 TEM 作为标样。分析流程见文献(Harris *et al.*, 2004)。

为了减少继承铅、铅丢失等对年龄的影响,在$^{207}Pb/^{235}U$-$^{206}Pb/^{238}U$ 图中谐和度低于 90% 的年龄数据将剔除(Liang *et al.*, 2006)。锆石 Ce^{4+}/Ce^{3+} 据锆石微量元素含量及岩体微量元素含量计算(Ballard *et al.*, 2002; Liang *et al.*, 2006)。

罗卜岭斑岩铜钼矿床矿化斑岩的锆石 U-Pb 年龄分别见表 2、表 3、表 4。

5 讨论

5.1 矿化岩体的形成时代及岩浆活动期次

晚期黑云母花岗闪长斑岩 LBL-132 锆石 LA-ICP-MS U-Pb 年龄 25 个分析点中,2 个点的谐和度低于 90%,在计算年龄时被排除,其余 23 个分析点年龄在 90.8 ~ 104.6Ma 之间。用 Isoplot 软件计算加权平均年龄为 97.6 ± 2.1Ma,MSWD = 6.00(图 4a)。

早期黑云母花岗闪长斑岩 LBL-81 共作 25 颗锆石 LA-ICP-MS U-Pb 年龄分析,除 1 个点的谐和度低于 90%,在计算年龄时被排除外,其余 24 个点的年龄变化范围在 98.4 ~ 108.4Ma 之间。用 Isoplot 软件计算加权平均年龄为 103.0 ± 0.9Ma, MSWD = 1.00(图 4b)。

角闪黑云母花岗闪长斑岩 LBL-203 的 LA-ICP-MS U-Pb 年龄变化很小。在 23 个分析点中,除 3 个谐和度低于 90% 而在计算年龄时被排除外,其余 20 个点的年龄范围在 101.8 ~ 109.2Ma 之间。用 Isoplot 软件计算加权平均年龄为 103.7 ± 1.2Ma,MSWD = 0.33(图 4c)。

测试的锆石主要为长柱状,晶形较好,Th/U 比值较大,在 0.25 ~ 0.98 之间(表 2、表 3、表 4);锆石 CL 图像韵律环带发育(图 5)。这表明锆石主要是岩浆结晶作用过程中形成的。锆石的 U-Pb 同位素体系的封闭温度较高(750 ± 50℃),抗后期干扰事件能力强,岩体锆石的 U-Pb 年龄可以代表岩体的结晶年龄。因此,罗卜岭斑岩铜钼矿床矿化花岗闪长斑岩锆石年龄代表成矿斑岩岩浆的侵位时代。

角闪黑云母花岗闪长斑岩 LBL-203 锆石 LA-ICP-MS U-Pb 年龄(103.7 ± 1.2Ma,MSWD = 0.33)和早期黑云母花岗闪长斑岩 LBL-81 锆石 LA-ICP-MS U-Pb 年龄(103.0 ± 0.9Ma, MSWD = 1.00)在误差范围内基本一致,表明其形成于同一期岩浆作用。晚期黑云母花岗闪长斑岩 LBL-132 的锆石 LA-ICP-MS U-Pb 年龄(97.6 ± 2.1Ma,MSWD = 6.00)小于角闪黑云母花岗闪长斑岩和早期黑云母花岗闪长斑岩的锆石 LA-ICP-MS U-Pb 年龄,这一结果与我们观察到的晚期黑云母花岗闪长斑岩包裹早期黑云母花岗闪长斑岩的地质现象一致。据罗卜岭赋矿斑岩锆石 LA-ICP-MS U-Pb 年龄差异、两期黑云母花岗闪长斑岩接触关系及矿物组成的差异,我们认为罗卜岭斑岩铜钼矿床至少发生了两期岩浆活动:早期侵入时代在 103Ma 左右,主要形成角闪黑云母花岗闪长斑岩及黑云母花岗闪长斑岩;晚期岩浆侵入时代在 97Ma 左右,主要形成黑云母花岗闪长斑岩。

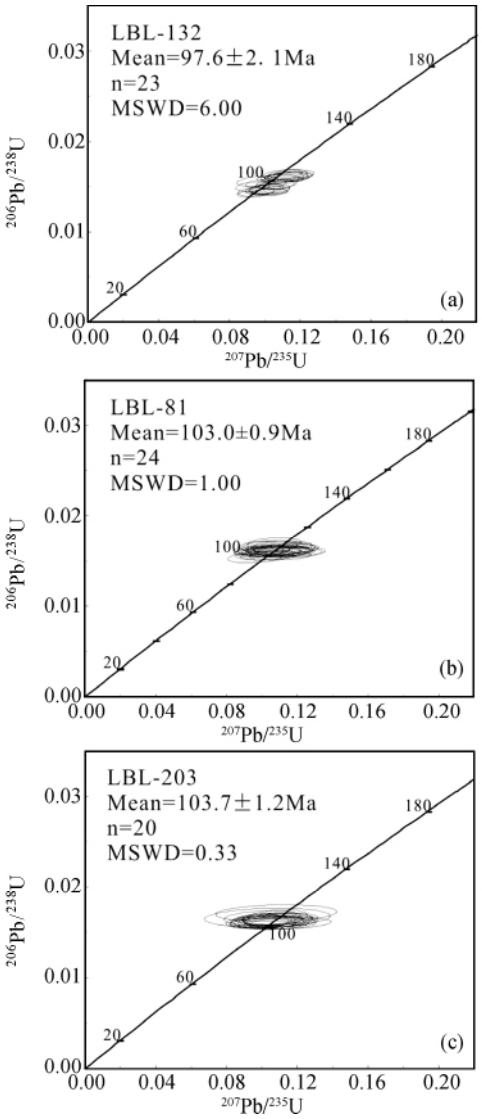

图 4 罗卜岭斑岩铜钼矿床矿化斑岩锆石 LA-ICP-MS U-Pb 年龄谐和图

Fig. 4 Concordia plots showing the zircon U-Pb analyses of the Luoboling mineralized porphyries

野外观察显示,罗卜岭两期斑岩都发育有斑岩型矿床典型的蚀变分带并伴随强烈矿化,显示晚期斑岩发生了成矿作用。早期斑岩锆石 LA-ICP-MS U-Pb 年龄和梁清玲等(2012)的辉钼矿 Re-Os 年龄(104.9 ± 1.6Ma)在误差范围内一致,表明早期斑岩也发生了成矿作用。据此,我们初步认为罗卜岭斑岩矿床可能发生了两期斑岩矿床成矿事件,早期约在

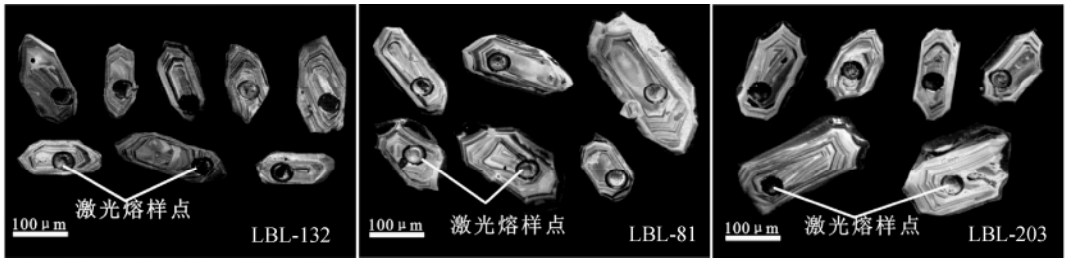

图 5　罗卜岭矿化斑岩锆石 CL 图

Fig. 5　CL images of analyzed zircon grains from the Luoboling ore-bearing porphyries

103Ma 左右,晚期在 97Ma 左右。

5.2　岩浆特征及成因

斑岩铜金矿床成矿岩浆氧逸度一般较高(Sillitoe, 1997; Mungall, 2002; Sun *et al.*, 2004; Liang *et al.*, 2006, 2009)。高氧逸度岩浆中的硫主要为氧化硫,有利于岩浆中的成矿元素在岩浆熔融及分异结晶过程中发生富集,而锆石 Ce^{4+}/Ce^{3+} 比值可反映岩浆氧逸度相对高低,可作为区分成矿岩体与非成矿岩体的标志(Ballard *et al.*, 2002; Liang *et al.*, 2006):智利的邱吉卡玛塔斑岩铜矿成矿斑岩锆石 Ce^{4+}/Ce^{3+} 比值大于 300,而不含矿的则低于 300(Ballard *et al.*, 2002);西藏的玉龙成矿带成矿岩体与非成矿岩体锆石 Ce^{4+}/Ce^{3+} 比值也明显不同(Liang *et al.*, 2006; 梁华英等, 2010)。

罗卜岭斑岩铜钼矿床早期角闪黑云母花岗闪长斑岩 LBL-203 锆石 Ce^{4+}/Ce^{3+} 比值在 98 ~ 2461 之间,平均值为 770(表 4);早期黑云母花岗闪长斑岩 LBL-81 锆石 Ce^{4+}/Ce^{3+} 比值在 113 ~ 3576 之间,平均值为 630(表 3);晚期黑云母花岗闪长斑岩 LBL-132 锆石 Ce^{4+}/Ce^{3+} 比值在 176 ~ 1642 之间,平均值为 768(表 2),而区内才溪岩体、英安玢岩及四坊岩体锆石 Ce^{4+}/Ce^{3+} 平均值分别为: 182、440、577(另文发表)。区内成矿岩体锆石 Ce^{4+}/Ce^{3+} 比值高于非成矿岩体锆石 Ce^{4+}/Ce^{3+} 比值,表明成矿岩体岩浆具较高的氧逸度。这与 Ballard *et al.*(2002) 和 Liang *et al.*(2006) 所得的结论一致。罗卜岭斑岩矿床两期成矿斑岩基质中普遍发育岩浆期的硬石膏,并在钾化阶段发育石英-钾长石-硬石膏脉,也表明成矿岩浆具高的氧逸度。

洋壳俯冲过程中脱水,在大陆边缘形成高氧化岩浆,因此,与洋壳俯冲有关的岩浆多具较高氧逸度(Ballhaus, 1993; Brandon and Draper, 1996; Parkinson and Arculus, 1999; Sun *et al.*, 2007)。罗卜岭斑岩铜钼矿床矿化斑岩的高氧逸度较高,表明其可能与洋壳俯冲有关。考虑到中国东部在侏罗纪之前为活动大陆边缘(Xu *et al.*, 1987; Zhou and Li, 2000; Zhu *et al.*, 2005; Zhou *et al.*, 2006),而白垩纪古太平洋板块俯冲方向的改变与中国东部大型构造事件密切相关(Sun *et al.*, 2007)。古太平洋板块在 125 ~ 120Ma 时俯冲方向发生变化(Koppers *et al.*, 2001, 2003),由 SW 方向俯冲转为 NWW 方向俯冲(Sun *et al.*, 2007)。而罗卜岭斑岩铜钼矿床成岩成矿时代在 103.6 ~ 97.6Ma 之间。据此我们认为罗卜岭斑岩铜钼矿床及其所在的紫金山浅成低温-斑岩矿床成矿系统主要与古太平洋板块 NWW 方向俯冲有关,可能是古太平洋板块俯冲脱水导致上部地幔楔部分熔融的产物。

6　结论

(1) 罗卜岭斑岩铜钼矿床发生过两期岩浆活动: 早期斑岩形成时代在 103Ma 左右,主要形成角闪黑云花岗闪长斑岩及黑云母花岗闪长斑岩; 晚期斑岩形成时代在 97Ma 左右,主要形成黑云母花岗闪长斑岩。罗卜岭斑岩铜钼矿床可能发生了两期斑岩成矿事件。

(2) 罗卜岭斑岩铜钼矿床早晚两期成矿岩浆的 Ce^{4+}/Ce^{3+} 比值较大,岩石中普遍发育岩浆期石膏和钾化阶段的石英-钾长石-硬石膏脉,表明罗卜岭斑岩铜钼矿床的成矿岩浆为高氧逸度岩浆,区域内的高氧逸度岩浆更有利于成矿。罗卜岭高氧逸度成矿岩浆的形成可能和古太平洋板块向 NWW 方向俯冲有关。

References

Ballard JR, Palin JM and Campbell IH. 2002. Relative oxidation states of magmas inferred from Ce(IV)/Ce(III) in zircon: Application to porphyry copper deposits of northern Chile. Contribution to Mineralogy and Petrology, 144(3): 347 - 364

Ballhaus C. 1993. Redox states of lithospheric and asthenospheric upper-mantle. Contributions to Mineralogy and Petrology, 114(3): 331 - 348

Bowen R and Gunatilaka A. 1977. Copper: Its Geology and Economics. London: Applied Science Publishers Ltd, 1 - 150

Brandon AD and Draper DS. 1996. Constraints on the origin of the oxidation state of mantle overlying subduction zones: An example from Simcoe, Washington, USA. Geochimica et Cosmochimica Acta, 60(10): 1739 - 1749

Bureau of Geology and Mineral Resources of Fujian Province (BGMRF). 1985. Regional Geology of Fujian Province (Attached Figure 1: Geological Map of Fujian Province, Peoples Republic of China 1∶500000). Beijing: Geological Publishing House (in Chinese)

Chen J, Chen YJ, Zhong J, Sun Y, Li J and Qi JP. 2011. Fluid inclusion study of the Wuziqilong Cu deposit in the Zijinshan ore field, Fujian Province. Acta Petrologica Sinica, 27(5): 1425 - 1438 (in Chinese with English abstract)

Chen YJ and Fu SG. 1992. Gold Mineralization in West Henan. Beijing: Seismological Press, 1 – 234 (in Chinese with English abstract)
Chen YJ. 1997. Mineralization during collisional orogenesis and its control of the distribution of gold and other deposits in Junggar orogen, Xinjiang, China. Acta Geologica Sinica, 71(1): 69 – 79
Chen YJ. 2000. Progress in the study of Central Asia type orogenesis-metallogenesis in Northwest China. Geological Journal of China Universities, 6(1): 17 – 22 (in Chinese with English abstract)
Chen YJ, Li C, Zhang J, Li Z and Wang HH. 2000. Sr and O isotopic characteristics of porphyries in the Qinling molybdenum deposit belt and their implication to genetic mechanism and type. Science in China (Series D), 43(Suppl.): 82 – 94
Chen YJ. 2002. Several important problems in study of regional metallogenesis in China: Their relationship to continental collision. Earth Science Frontiers, 9(4): 319 – 328 (in Chinese)
Chen YJ, Pirajno F and Sui YH. 2004. Isotope geochemistry of the Tieluping silver-lead deposit, Henan, China: A case study of orogenic silver-dominated deposits and related tectonic setting. Mineralium Deposita, 39(5 – 6): 560 – 575
Chen YJ, Chen HY, Zaw K, Pirajno F and Zhang ZJ. 2007. Geodynamic settings and tectonic model of skarn gold deposits in China: An overview. Ore Geology Reviews, 31(1 – 4): 139 – 169
Chen YJ, Ni P, Fan HR, Pirajno F, Lai Y, Su WC and Zhang H. 2007. Diagnostic fluid inclusions of different types hydrothermal gold deposits. Acta Petrologica Sinica, 23(9): 2085 – 2108 (in Chinese with English abstract)
Chen YJ and Li N. 2009. Nature of ore-fluids of intracontinental intrusion-related hypothermal deposits and its difference from those in island arcs. Acta Petrologica Sinica, 25(10): 2477 – 2508 (in Chinese with English abstract)
Chen YJ, Pirajno F, Wu G, Qi JP and Xiong XL. 2012. Epithermal deposits in North Xinjiang, NW China. International Journal of Earth Sciences, 101(4): 889 – 917
Chen YJ, Zhang C, Li N, Yang YF and Deng K. 2012. Geology of the Mo deposits in Northeast China. Journal of Jilin University (Earth Science Edition), 42(5): 1223 – 1268 (in Chinese with English abstract)
Chen YJ. 2013. The development of continental collision metallogeny and its application. Acta Petrologica Sinica, 29(1): 1 – 17 (in Chinese with English abstract)
Harris AC, Allen CM, Bryan SE, Campbell IH, Holcombe RJ and Plain MJ. 2004. ELA-ICP-MS U-Pb zircon geochronology of regional volcanism hosting the Bajo de la Alumbrera Cu-Au deposit: Implications for porphyry-related mineralization. Mineralium Deposita, 39(1): 46 – 67
Hua RM, Hu JH, Huang YS and Li ZM. 1998. Fluid migration-reaction model of Zijinshan deposit as traced by variation of oxygen isotope compositions. Geochimica, 27(2): 186 – 195 (in Chinese with English abstract)
Hua RM, Lu JJ, Chen PR, Li XF, Liu XD and Zhang WL. 2002. The late Mesozoic porphyry-epithermal gold (copper) system and its ore-forming fluid in the East of China. Progress in Nature Science, 12(3): 240 – 244 (in Chinese)
Hou ZQ, Mo XX, Gao YF, Qu XM and Meng XJ. 2003. Adakite, a possible host rock for porphyry copper deposits: Case studies of porphyry copper belt in Tibetan Plateau and in Northern Chile. Mineral Deposits, 22(1): 1 – 12 (in Chinese with English abstract)
Koppers AAP, Morgan JP, Morgan JW and Staudigel H. 2001. Testing the fixed hotspot hypothesis using $^{40}Ar/^{39}Ar$ age progressions along seamount trails. Earth and Planetary Science Letters, 185(3 – 4): 237 – 252
Koppers AAP, Staudigel H and Duncan RA. 2003. High-resolution $^{40}Ar/^{39}Ar$ dating of the oldest oceanic basement basalts in the western Pacific basin. Geochemistry, Geophysics, Geosystems, 4(11): 8914
Li N, Chen YJ, Zhang H, Zhao TP, Deng XH, Wang Y and Ni ZY. 2007. Molybdenum deposits in East Qinling. Earth Science Frontiers, 14(5): 186 – 198 (in Chinese with English abstract)
Liang HY, Campbell IH and Allen CM. 2006. Zircon Ce^{4+}/Ce^{3+} ratios and ages for Yulong ore-bearing porphyry in eastern Tibet. Mineralium Deposita, 41(2): 152 – 159
Liang HY, Sun WD, Su WC and Zartman RE. 2009. Porphyry copper-gold mineralization at Yulong, China, promoted by decreasing redox potential during magnetite alteration. Economic Geology, 104(4): 587 – 596
Liang HY, Wei QR, Xu JF, Hu GQ and Allen C. 2010. Study on zircon LA-ICP-MS U-Pb age of skarn Cu mineralization related intrusion in the southern margin of the Gangdese ore belt, Tibet and its geological implication. Acta Petrologica Sinica, 26(6): 1692 – 1698 (in Chinese with English abstract)
Liang QL, Jiang SH, Wang SH, Li C and Zeng FG. 2012. Re-Os dating of molybdenite from the Luoboling porphyry Cu-Mo deposit in the Zijinshan ore field of Fujian province and its geological significance. Acta Geologica Sinica, 86(7): 1113 – 1118 (in Chinese with English abstract)
Mao JR, Tao KY, Lee CY, Xie FG and Xu NZ. 2002. Geochronology and geochemical characteristics in Late Mesozoic Sifang pluton, southwestern Fujian, and their significance. Acta Petrologica Siaica, 18(4): 449 – 458 (in Chinese with English abstract)
Mitchell AHG. 1973. Metallogenic belts and angle of dip of Benioff zones. Nature, 245(143): 49 – 52
Mungall JE. 2002. Roasting the mantle: Slab melting and the genesis of major Au and Au-rich Cu deposits. Geology, 30(10): 915 – 918
Parkinson IJ and Arculus RJ. 1999. The redox state of subduction zones: Insights from arc-peridotites. Chemical Geology, 160(4): 409 – 423
Qi JP, Chen YJ and Pirajno F. 2005. Geological characteristics and tectonic setting of the epithermal deposits in the Northeast China. Journal of Mineralogy and Petrology, 2005, 25(2): 47 – 59 (in Chinese with English abstract)
Richards JP. 2003. Tectono-magmatic precursors for porphyry Cu-(Mo-Au) deposit formation. Economic Geology, 98(8): 1515 – 1533
Richards JP. 2009. Postsubduction porphyry Cu-Au and epithermal Au deposits: Products of remelting of subduction-modified lithosphere. Geology, 37(3): 247 – 250
Rui ZY, Hou ZQ, Li GM, Zhang LS and Tang SH. 2006. Subduction, collision, deep fracture, adakite and porphyry copper deposits. Geology and Prospecting, 42(1): 1 – 6 (in Chinese with English abstract)
Seedorff E, Dilles JH, Proffett JM, Einaudi MT, Zurcher L, Stavast WJA, Johnson DA and Barton MD. 2005. Porphyry deposits: Characteristics and origin of hypogene features. In: Hedenquist JW, Thompson JFH and Goldfarb RJ (eds.). Economic Geologists 100th Anniversary Volume, Littleton: Society of Economic Geologists, 251 – 298
Sillitoe RH. 1972. A plate tectonic model for the origin of porphyry copper deposits. Economic Geology, 67(2): 184 – 197
Sillitoe RH. 1997. Characteristics and controls of the largest porphyry copper-gold and epithermal gold deposits in the circum-Pacific region. Australian Journal of Earth Sciences, 44(3): 373 – 388
Sillitoe RH. 2010. Porphyry copper systems. Economic Geology, 105(1): 3 – 41
Stern CR, Funk JA, Skewes MA and Arévalo A. 2007. Magmatic anhydrite in plutonic rocks at the EL Teniente Cu-Mo deposit, Chile, and the role of sulfur- and copper-rich magmas in its formation. Economic Geology, 102(7): 1335 – 1344
So CS, Zhang DQ, Yun ST and Li DX. 1997. Alteration-mineralization zoning and fluid inclusions of the high sulfidation epithermal Cu-Au mineralization at Zijinshan, Fujian Province, China. Economic Geology, 93(7): 961 – 980
Sun WD, Arculus RJ, Kamenetsky VS and Binns RA. 2004. Release of gold-bearing fluids in convergent margin magmas prompted by magnetite crystallization. Nature, 431(7011): 975 – 978
Sun WD, Ding X, Hu YH and Li XH. 2007. The golden transformation of Cretaceous plate subduction in the west Pacific. Earth and Planetary Science Letters, 262(3 – 4): 533 – 542
Wang SH, Pei RF, Zeng XH, Qiu XP and Wei M. 2009. Metallogenic series and model of the Zijinshan mining field. Acta Geologica Sinica, 83(2): 145 – 157 (in Chinese with English abstract)
Xu JW, Zhu G, Tong WX, Cui KR and Lin Q. 1987. Formation and

evolution of the Tancheng-Lujiang wrench fault system: A major shear system to the northwest of the Pacific Ocean. Tectonophysics, 134(4): 273 – 310

Xue K and Ruan SK. 2008. Geological characteristics and genesis of the Luobuling copper (molybdenum) deposit in Zijinshan ore-field, Fujian. Resources Environment and Engineering, 22(5): 491 – 496 (in Chinese with English abstract)

Zhang DQ, Li DX, Zhao YM, Chen JH, Li ZL and Zhang KY. 1992. Alteration and Mineralization Zoning of the Zijinshan Copper-Gold Deposit. Beijing: Geological Publishing House, 1 – 77 (in Chinese)

Zhang DQ, She HQ, Yan SH and Xu WY. 2001. Geochemistry of Mesozoic magmatites in the Zijinshan region and implication on regional tectonic inversion. Geological Review, 47(6): 608 – 616 (in Chinese with English abstract)

Zhang DQ, She HQ, Li DX and Feng CY. 2003. The porphyry-epithermal metallogenic system in the Zijinshan region, Fujian Province. Acta Geologica Sinica, 77(2): 253 – 261 (in Chinese with English abstract)

Zhang DQ, Feng CY, Li DX, She HQ and Dong YJ. 2005. The evolution of ore-forming fluid in the porphyry-epithermal metallogenic system of Zijinshan area. Acta Geoscientica Sinica, 26(2): 127 – 136 (in Chinese with English abstract)

Zhao XL, Mao JR, Chen R, Xu NZ, Zeng QT and Ye HM. 2007. Zircon SHRIMP age and geochemical characteristics of the Caixi pluton in southwestern Fujian Province. Acta Petrologica et Mineralogica, 26(3): 223 – 231 (in Chinese with English abstract)

Zhao XL, Mao JR, Chen R and Xu NZ. 2008. SHRIMP zircon dating of the Zijinshan pluton in southwestern Fujian and its implications. Geology in China, 35(4): 590 – 597 (in Chinese with English abstract)

Zheng YY, Wang BS, Fan ZH and Zhang HP. 2002. Analysis of tectonic evolution in the eastern section of the Gangdise Mountains, Tibet and the metallogenic potentialities of copper gold poly metal. Geological Science and Technology Information, 21(2): 55 – 60 (in Chinese with English abstract)

Zhou XM and Li WX. 2000. Origin of late Mesozoic igneous rocks in southeastern China: Implications for lithosphere subduction and underplating of mafic magmas. Tectonophysics, 326(3 – 4): 269 – 287

Zhou XM, Sun T, Shen WZ, Shu LS and Niu YL. 2006. Petrogenesis of Mesozoic granitoids and volcanic rocks in South China: A response to tectonic evolution. Episodes, 29(1): 26 – 33

Zhong J, Chen YJ, Chen J, Li J, Qi JP and Dai MC. 2011. Fluid inclusion study of the Luoboling porphyry Cu-Mo deposit in the Zijinshan ore field, Fujian Province. Acta Petrologica Sinica, 27(5): 1410 – 1424 (in Chinese with English abstract)

Zhu G, Wang YS, Liu GS, Niu ML, Xie CL and Li CC. 2005. $^{40}Ar/^{39}Ar$ dating of strike-slip motion on the Tan-Lu fault zone, East China. Journal of Structural Geology, 27(8): 1379 – 1398

附中文参考文献

陈静，陈衍景，钟军，孙艺，李晶，祁进平. 2011. 福建省紫金山矿田五子骑龙铜矿床流体包裹体研究. 岩石学报，27(5): 1425 – 1438

陈衍景，富士谷. 1992. 豫西金矿成矿规律. 北京: 地震出版社，1 – 234

陈衍景. 2000. 中国西北地区中亚型造山-成矿作用的研究意义和进展. 高校地质学报，6(1): 17 – 22

陈衍景. 2002. 中国区域成矿研究的若干问题及其与陆-陆碰撞的关系. 地学前缘，9(4): 319 – 326

陈衍景，倪培，范洪瑞，Pirajno F，赖勇，苏文超，张辉. 2007. 不同类型热液金矿系统的流体包裹体特征. 岩石学报，23(9): 2085 – 2108

陈衍景，李诺. 2009. 大陆内部浆控高温热液矿床成矿流体性质及其与岛弧区同类矿床的差异. 岩石学报，25(10): 2477 – 2508

陈衍景，张成，李诺，杨永飞，邓轲. 2012. 中国东北钼矿床地质. 吉林大学学报(地球科学版)，42(5): 1223 – 1268

陈衍景. 2013. 大陆碰撞成矿理论的创建及应用. 岩石学报，29(1): 1 – 17

福建省地质矿产局. 1985. 福建省区域地质志(附图之一: 中华人民共和国福建省地质图 1∶500000). 北京: 地质出版社

华仁民，胡金化，黄耀生，李振敏. 1998. 福建紫金山矿床流体运移-反应模式及其氧同位素示踪研究. 地球化学，27(2): 186 – 195

华仁民，陆建军，陈培荣，李晓峰，刘晓东，张文兰. 2002. 中国东部晚中生代斑岩-浅成热液金(铜)矿体系及其成矿流体. 自然科学进展，12(3): 240 – 244

侯增谦，莫宣学，高永丰，曲晓明，孟祥金. 2003. 埃达克岩: 斑岩铜矿的一种可能的重要含矿母岩——以西藏和智利斑岩铜矿为例. 矿床地质，22(1): 1 – 12

李诺，陈衍景，张辉，赵太平，邓小华，王运，倪智勇. 2007. 东秦岭斑岩钼矿带的地质特征和成矿构造背景. 地学前缘，14(5): 186 – 198

梁华英，魏启荣，许继峰，胡光黔，Allen C. 2010. 西藏冈底斯矿带南缘矽卡岩型铜矿床含矿岩体锆石 U-Pb 年龄及意义. 岩石学报，26(6): 1692 – 1698

梁清玲，江思宏，王少怀，李超，曾法刚. 2012. 福建紫金山矿田罗卜岭斑岩型铜钼矿床辉钼矿 Re-Os 定年及地质意义. 地质学报，86(7): 1113 – 1118

毛建仁，陶奎元，李寄嵎，谢方贵，许乃政. 2002. 闽西南晚中生代四方岩体同位素年代学、地球化学及其构造意义. 岩石学报，18(4): 449 – 458

祁进平，陈衍景，Pirajno F. 2005. 东北地区浅成低温热液矿床的地质特征和构造背景. 矿物岩石，25(2): 47 – 59

芮宗瑶，侯增谦，李光明，张立生，王龙生，唐索寒. 2006. 俯冲、碰撞、深断裂和埃达克岩与斑岩铜矿. 地质与勘探，42(1): 1 – 6

王少怀，裴荣富，曾宪辉，邱小平，魏民. 2009. 再论紫金山矿田成矿系列与成矿模式. 地质学报，83(2): 145 – 157

薛凯，阮诗昆. 2008. 福建紫金山矿田罗卜岭铜(钼)矿床地质特征及成因探讨. 资源环境与工程，22(5): 491 – 496

张德全，李大新，赵一鸣，陈景河，李子林，张克尧. 1992. 紫金山铜金矿床蚀变及矿化分带. 北京: 地质出版社，1 – 77

张德全，佘宏全，阎升好，徐文艺. 2001. 福建紫金山地区中生代构造环境转换的岩浆岩地球化学证据. 地质论评，47(6): 608 – 616

张德全，佘宏全，李大新，丰成友. 2003. 紫金山地区的斑岩-浅成热液成矿系统. 地质学报，77(2): 253 – 261

张德全，丰成友，李大新，佘宏全，董英君. 2005. 紫金山地区斑岩-浅成热液成矿系统的成矿流体演化. 地球学报，26(2): 127 – 136

赵希林，毛建仁，陈荣，许乃政，曾庆涛，叶海敏. 2007. 闽西南地区才溪岩体锆石 SHRIMP 定年及其地球化学特征. 岩石矿物学杂志，26(3): 223 – 231

赵希林，毛建仁，陈荣，许乃政. 2008. 闽西南地区紫金山岩体锆石 SHRIMP 定年及其地质意义. 中国地质，35(4): 590 – 597

郑有业，王保生，樊子晖，张华平. 2002. 西藏冈底斯东段构造演化及铜金多金属成矿潜力分析. 地质科技情报，21(2): 55 – 60

钟军，陈衍景，陈静，李晶，祁进平，戴茂昌. 2011. 福建省紫金山矿田罗卜岭斑岩型铜钼矿床流体包裹体研究. 岩石学报，27(5): 1410 – 1424